Rational Synthetic Strategy. From Layered Structure to MnO_2 Nanotubes

Xun Wang and Yadong Li*
Department of Chemistry and the Key Laboratory of Atomic & Molecular Nanosciences (Ministry of Education, China),
Tsinghua University, Beijing, 100084, P. R. China

(Received September 29, 2003; CL-030914)

In this manuscript, a rational synthetic strategy from layer structure to nanotubes has been developed in the synthesis of δ-MnO_2 single crystal nanotubes by employing layered α-$NaMnO_2$ as precursors through a controlled hydrothermal intercalation process.

Previous studies suggest that substances that possess layer structures might be able to form nanotubes under favorable conditions.[1–6] This concept has been inspiring us to explore general synthetic strategy to nanotubes from artificial or natural layer structures.[4,6–8] In our recent synthesis of MnO_2 nanowires/nanorods,[9,10] it has been found that layer-structured curling δ-MnO_2 can serve as intermediate in the formation process of MnO_2 nanowries/nanorods with different crystal structures.[10] So we believe that under favorable conditions, δ-MnO_2 and other compounds possessing similar layer structures can be prepared as nanotubes, and the case is how to design a rational process. Herein we demonstrate a successful example from layered α-$NaMnO_2$ to δ-MnO_2 single crystal nanotubes through a controlled hydrothermal intercalation way.

As shown in Figure 1, δ-MnO_2 has a 2-D layered structure that consists of edge-shared $[MnO_6]$ octahedra with cations and water molecular occupying the interlayer region. Based on our previous studies, the $[MnO_6]$ octahedral layers could be easily exfoliated and tend to curl under hydrothermal conditions, which have provided the possibility for the formation of δ-MnO_2 nanotubes.[10] Rational precursors and favorable conditions may facilitate this formation process. Among the numerous manganese oxides, α-$NaMnO_2$ (sodium manganese oxide) is layered and adopts a monoclinic distortion of the $LiCoO_2$ structure caused by the Jahn–Teller activity of Mn^{3+}. Na^+ ions reside between edge-shared $[MnO_6]$ octahedra layers in $NaMnO_2$ (Figure 1a).[11,12] The strong static interaction between the Na^+ ions and $[MnO_6]$ units holds the layers together tightly and makes it impossible for these layers to roll up into nanotubes. However, the layer-structured α-$NaMnO_2$ has proven to be an ideal precursor for the formation of δ-MnO_2 nanotubes.

Under a neutral pH condition, Mn^{3+} is unstable and disproportionation reaction will occur,

$$Mn^{3+} \rightarrow Mn^{2+} + MnO_2$$
$$(E^\circ = +0.56\,V;\ \Delta G^\circ = -54.04\,kJ{\cdot}mol^{-1})$$

Along with this process, Na^+ ions will be released, and the $NaMnO_2$ can be gradually intercalated by water molecule with part of the Mn^{3+} transformed into Mn^{4+},[11] which will in situ adopt $[MnO_6]$ octahedra to form manganese oxides layers with intercalated H_2O. As a result, the interlayer distance will be enlarged, so the strong static interaction between the MnO_6 octahedra sheets would be weakened to some extend, which might lower the energy barrier in turning into tubular morphology, and thus greatly increase the possibility for the formation of δ-MnO_2 nanotubes.

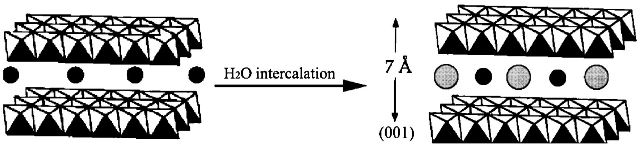

(a) (b)

Figure 1. Layer structure of α-$NaMnO_2$ (a) and δ-MnO_2 (b); gray shaded circles = H_2O, dark circles = Na ions;

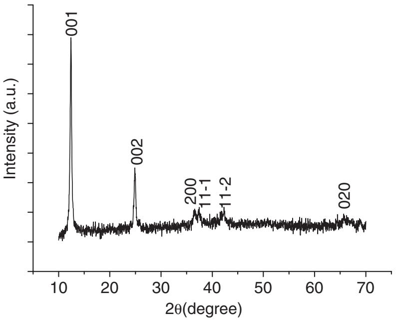

Figure 2. XRD patterns of the δ-MnO_2 nanotubes.

The designed synthetic process was performed under hydrothermal conditions. In a typical synthesis, 0.3 g $NaMnO_2$[12,13] was dispersed into 30-mL diluted water, then the mixture was transferred into a 40-mL Teflon-lined autoclave, sealed, and kept at 120–140 °C for about 4 days. Then the autoclave was allowed to cool to room temperature on standing. The as-obtained black precipitates were filtered, washed with diluted water to remove ions possibly remnant in the final products. and dried at 80 °C in air.

The phase purity of the samples has been characterized on a Brucker D8-advance X-ray powder diffractometer with Cu Kα radiation ($\lambda = 1.5418$ Å). As shown in Figure 2, all the reflections of the XRD patterns can be readily indexed to a pure monoclinic phase [space group $C2/m$ (12)] of δ-MnO_2 with lattice constants $a = 5.149$ Å, $b = 2.843$ Å, and $c = 7.176$ Å (JCPDS 80-1098). The peaks at 2θ values of 12.38, 24.88, 37.4, 42.58, and 66.12 degrees correspond to the crystal planes of 001, 002, 200, 112, and 020 of crystalline δ-MnO_2, respectively. The d value of the 001 peak can be calculated to be about 0.7 nm, corresponding to the (001) plane spacing of δ-MnO_2. All the information from this XRD pattern indicates that pure phase δ-MnO_2 could be obtained under current experimental conditions.

TEM analysis provides further insight into the morphology and microstructure details of the as-obtained δ-MnO_2 products.

As shown in Figures 3a–3c, all the samples dispersed on the copper grids show nanotube morphologies with diameters 10–20 nm and length up to several μm. Further magnified images of these nanotubes (Figures 3b and 3c) reveal their tubular structures with open ends. It is also interesting to find that these nanotubes tend to aggregate together to form cross-linked structures or bundles (Figures 3a and 3b).

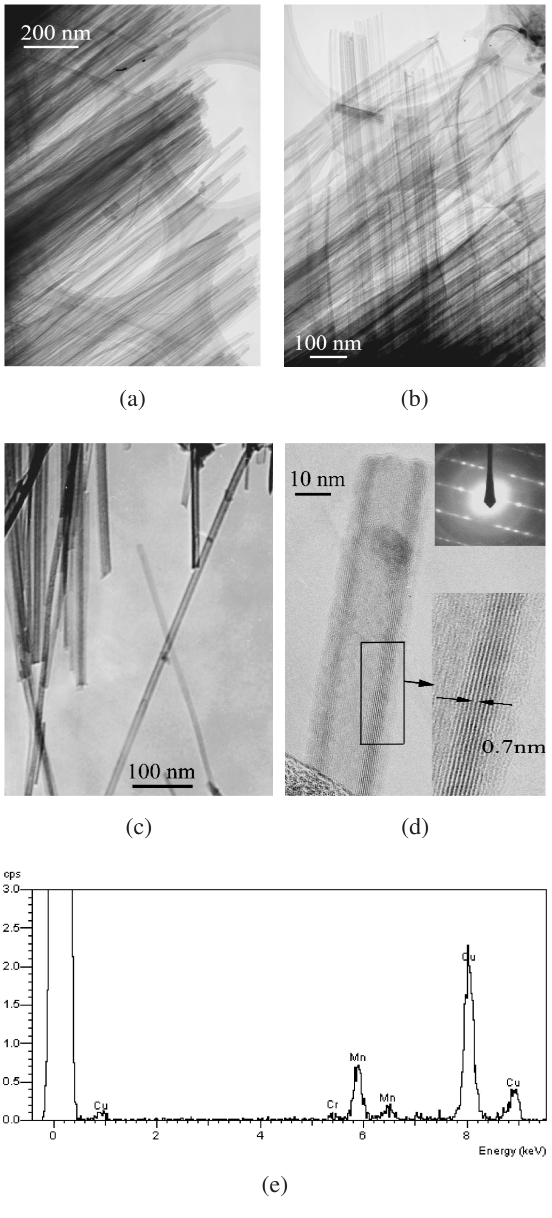

(a) (b)

(c) (d)

(e)

Figure 3. (a), (b), (c); Low magnification TEM images of δ-MnO_2 nanotubes; (d), high resolution TEM image of an individual δ-MnO_2 nanotube; Inset, electron diffraction patterns of the individual δ-MnO_2 nanotube shown in (d) (right upper); higher magnification of one-side wall of the individual δ-MnO_2 nanotube shown in (d) (right lower); (e), EDAX spectrum of the individual δ-MnO_2 nanotube shown in (d).

HRTEM analysis has provided more detailed structure information on these nanotubes. Figure 3d shows an individual open-end δ-MnO_2 nanotube with diameter ca. 20 nm. Further magnification clearly shows that its wall contains about 10 layers (Figure 3d inset, right lower). The interlayer spacing is calculated to be about 0.7 nm, which corresponds to the interlayer distance of (001) planes in δ-MnO_2 and coincides well with the XRD results. Electron diffraction patterns (Figure 3d inset, right upper), taken from the individual nanotube shown in Figure 3d, have revealed its single crystal nature. EDAX (Figure 3e), taken from the same nanotube shows that there are only Mn and O in the nanotubes, Na has not been detected in the sample.

Nitrogen-adsorption–desorption isotherms of these nanotubes (supporting materials) can be categorized as type IV with a distinct hysteresis loop observed in the range of 0.5–1.0 P/P_0, and corresponding Barrett–Joyner–Halenda (BJH) pore-size distribution plots (supporting materials) reveal a distribution centered at ca. 15 nm, which coincide well with the TEM observation.

The successful synthesis of δ-MnO_2 single crystal nanotubes may mean affluent physical and chemical contents. For example, because of the excellent ion-exchange ability of δ-MnO_2, these nanotubes can be further ion-exchanged into transitional metal ions (Li^+, Co^{2+}, Mg^{2+}, and Ni^{2+}, etc.)-doped ones, from which novel magnetic properties can be expected. Meanwhile, their unique tubular structural features make them ideal candidates as porous materials and find applications in lithium batteries, catalysts, molecular sieves, and gas mask fields, etc.

In this paper, δ-MnO_2 single-crystal nanotubes have been successfully synthesized in large scale through a rational layer-structure-to-nanotubes synthetic strategy. This strategy is based on the rational choice of precursors and growth conditions and can be readily extended to the synthesis of α-$NaMnO_2$-type layer structured nanotubes, such as clay, $NaFeO_2$, $Na_xCoO_2.yH_2O$, etc. We believe that the synthesis of bulk quantities of single-crystal nanotubes of MnO_2 and other technologically important transitional metal oxide materials will open up great opportunities for further fundamental studies and applications.

This work was supported by the NSFC, the Foundation for the Author of National Excellent Doctoral Dissertation of P. R. China, and the State Key Project of Fundamental Research for nanomaterials and nanostructures.

References

1 S. Iijima, *Nature*, **354**, 56 (1991).
2 R. Tenne, L. Margulis, M. Genut, and G. Hodes, *Nature*, **360**, 444 (1992).
3 M. E. Spahr, P. Bitterli, R. Nesper, M. Müller, F. Krumeich, and H. U. Nissen, *Angew. Chem., Int. Ed.*, **37**, 1263 (1998).
4 Y. D. Li, J. W. Wang, Z. X. Deng, Y. Y. Wu, X. M. Sun, D. P. Yu, and P. D. Yang, *J. Am. Chem. Soc.*, **123**, 9904 (2001).
5 L. M. Viculis, J. J. Mack, and R. B. Kaner, *Science*, **299**, 1361 (2003).
6 Y. D. Li, X. L. Li, R. R. He, J. Zhu, and Z. X. Deng, *J. Am. Chem. Soc.*, **124**, 1411 (2002).
7 X. M. Sun and Y. D. Li, *Chem.—Eur. J.*, **9**, 2229 (2003).
8 X. Chen, X. M. Sun, and Y. D. Li, *Inorg. Chem.*, **41**, 4524 (2002).
9 X. Wang and Y. D. Li, *J. Am. Chem. Soc.*, **124**, 2880 (2002).
10 X. Wang and Y. D. Li, *Chem.—Eur. J.*, **9**, 300 (2003).
11 X. Wang and Y. D. Li, *Chem. Commun.*, **2002**, 764.
12 S. Bach, J. P. Pereira-Ramos, and N. Baffier, *J. Solid State Chem.*, **120**, 70 (1995).
13 A. R. Armstrong and P. G. Bruce, *Nature*, **381**, 499 (1996).

Published on the web (Advance View) December 15, 2003; DOI 10.1246/cl.2004.48